Eur. Phys. J. A **21**, 437–443 (2004)
DOI 10.1140/epja/i2004-10008-x

THE EUROPEAN PHYSICAL JOURNAL A

Nuclear γ-radiation as a signature of ultra-peripheral ion collisions at the LHC

Yu.V. Kharlov[1] and V.L. Korotkikh[2,a]

[1] Institute for High Energy Physics, 142281 Protvino, Russia
[2] Scobeltsyn Institute of Nuclear Physics, Moscow State University, 119992 Moscow, Russia

Received: 10 February 2004 / Revised version: 9 March 2004 /
Published online: 14 September 2004 –
Communicated by W. Henning

Abstract. We study the peripheral ion collisions at LHC energies where a nucleus is excited to a discrete state and then emits γ-rays. Large nuclear Lorenz factors allow the observation of high-energy photons up to a few tens GeV and in the angular region of a few hundred micro-radians from the beam direction. These photons can be used to tagg events with particle production in the central rapidity region in ultra-peripheral collisions. To detect these photons it is necessary to have an electromagnetic detector in front of the zero-degree calorimeter in LHC experiments.

PACS. 25.75.-q Relativistic heavy-ion collisions – 25.75.Dw Particle and resonance production

Introduction

There are several reviews devoted to coherent $\gamma\gamma$ and γg interactions in very peripheral collisions at relativistic ion colliders [1–3]. The advantage of relativistic heavy-ion colliders is that the effective photon luminosity for two-photon physics is orders of magnitude higher than that available in e^+e^- machines. There have been many suggestions to use the electromagnetic interactions of nuclei to study production of meson resonances, Higgs bosons, Radions or exotic mesons. These interactions also probe fermion, vector meson or boson pair production, as well as investigate some new physics regions (see list in ref. [3]). The γg interactions will open a new area of nuclear physics such as the study of nuclear gluon distribution. It is also important for the knowledge of the details of medium effects in nuclear matter at the formation of the quark-gluon plasma [4]. These effects may be studied by photo-production of heavy quarks in virtual photon-gluon interactions [4–6].

For these investigations it is necessary to select processes with large impact parameters b of the colliding nuclei, $b > (R_1 + R_2)$, to exclude background from strong interactions. Note that some processes, like $\gamma\gamma$-fusion to Higgs bosons or Radions, are free from any problems caused by strong interactions of the initial state [7]. Therefore, we need an efficient trigger to distinguish $\gamma\gamma$ and γg interactions from others. G. Baur *et al.* [8] suggested to detect intact nuclei after the interaction. Evidently this is impossible in LHC experiments since nuclei fly into the beam pipe.

It is interesting to consider γ-rays emitted by the relativistic nuclei at LHC energies. This process was used for the possible explanation of the high-energy ($E_\gamma \geq 10^{12}$ eV) cosmic photon spectrum [9].

We had considered [10] the process $A + A \to A^* + A + e^+e^-, A^* \to A + \gamma'$, where a nucleus is excited by the electron (positron) $e^\pm + A \to e^{\pm'} + A^*$, and suggested to detect a nuclear γ radiation after the excitation of discrete nuclear levels [10]. These secondary photons have the energy of a few GeV and a narrow angular distribution close the beam direction due to a large Lorentz boost. The angular width is large enough for them to be detected in the electromagnetic zero-degree calorimeters (ZDC) of the future LHC experiments CMS or ALICE.

Now we calculate the production process of some system X_f in $\gamma\gamma$ fusion with simultaneous excitation of the discrete nuclear level. The nucleus retains its charge Z and mass A in this process. So we have a clear electromagnetic interaction of nuclei at any impact parameter. The nuclear γ radiation may be used as "event-by-event" criteria in these collisions.

In this work we consider the processes

$$^{16}\mathrm{O} +^{16} \mathrm{O} \to^{16} \mathrm{O} +^{16} \mathrm{O}^*(2^+, 6.92\ \mathrm{MeV}) + X_f,$$
$$^{16}\mathrm{O}^* \to^{16} \mathrm{O} + \gamma,$$
$$^{208}\mathrm{Pb} +^{208} \mathrm{Pb} \to^{208} \mathrm{Pb} +^{208} \mathrm{Pb}^*(3^-, 2.62\ \mathrm{MeV}) + X_f,$$
$$^{208}\mathrm{Pb}^* \to^{208} \mathrm{Pb} + \gamma,$$

where the ^{16}O and ^{208}Pb were taken since they are the lightest and heaviest ions in the LHC program. The trigger requirements will include a signal in the central rapidity

[a] e-mail: vlk@lav01.sinp.msu.ru

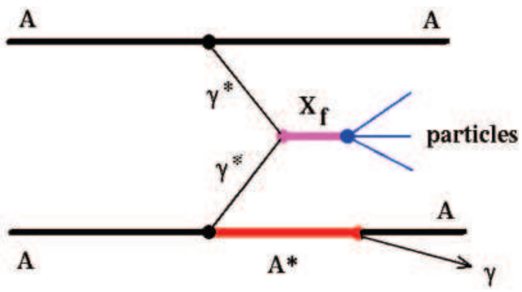

Fig. 1. Diagram of the process $A_1 + A_2 \to A_1^*(\lambda^P, E_0) + A_2 + X_f,\ A_1^* \to A_1 + \gamma$.

region of particles from X_f decay, a signal of photons in the electromagnetic detector in front of the zero-degree calorimeter and a veto signal of neutrons in the ZDC. We suggest to use the veto signal of neutrons in order to avoid the processes with nuclear decay into nucleon fragments.

The formalism of the considered process is presented in sect. 1. The nuclear form factors are calculated in sect. 2. The angular and energy distributions of secondary photons are in sect. 3. The cross-sections of η_c (2.979 GeV) production are presented in sect. 4 with and without nuclear excitation. Section 5 is our conclusion.

1 Formulae of nuclear excitation cross-section and photon luminosity in peripheral interactions

Let us consider the peripheral ion collision

$$A_1 + A_2 \to A_1^*(\lambda^P, E_0) + A_2 + X_f, \tag{1}$$

where X_f is the produced system in $\gamma^*\gamma^*$ fusion and A_1^* is an excited nucleus in a discrete nuclear state with spin-parity λ^P and energy E_0 (see fig. 1). Here the nuclei A_1 and A_2 have equal mass A and charge Z, only the nucleus A_1 is excited. We suppose that the reaction product X_f decay can be detected in the central rapidity region. The nuclear γ radiation $A_1^* \to A_1 + \gamma$ will be measured in the forward detectors as ZDC.

We use the quantum-mechanical plane-wave formalism [3,11] and the derivation of the equivalent photon approximation. This allows us to introduce the elastic and inelastic nuclear form factors for process (1). We take the formulae (19) and (21) in [3] :

$$\mathrm{d}\sigma_{A_1A_2\to A_1^*A_2X_f} = \int \frac{\mathrm{d}w_1}{w_1}\int\frac{\mathrm{d}w_2}{w_2} n_1(w_1)n_2(w_2)\ \cdot \cdot\,\mathrm{d}\sigma_{\gamma\gamma\to X_f}(w_1,w_2), \tag{2}$$

$$n_i(w_i) = \frac{\alpha}{\pi^2}\int \mathrm{d}^2 q_{i\perp}\int \mathrm{d}\nu_i \frac{1}{(q_i^2)^2}\ \cdot \cdot\,\mathrm{d}\left[2\frac{w_i^2 m_i^2}{P_i^2} W_{i,1}(\nu_i, q_i^2) + q_{i\perp}^2 W_{i,2}(\nu_i,q_i^2)\right], \tag{3}$$

where $W_{i,1}$ and $W_{i,2}$ are the Lorentz scalar functions. All kinematic variables have the same definitions as in [3].

For the "elastic" photon process $A_1A_2 \to A_1A_2X_f$ we have

$$W_1 = 0,\ W_2(\nu, q^2) = Z^2 F_{\mathrm{el}}^2(-q^2)\delta(\nu + q^2/2m). \tag{4}$$

So that [3]

$$n(w) = \frac{Z^2\alpha}{\pi^2}\int \mathrm{d}^2 q_\perp \frac{q_\perp^2}{(q^2)^2} F_{\mathrm{el}}^2(-q^2), \tag{5}$$

where $F_{\mathrm{el}}(q)$ is the nuclear form-factor with $F_{\mathrm{el}}(0) = 1$.

For the excitation of the nucleus to a discrete state with a spin λ and an energy E_0 ("inelastic" photon process $A_1A_2 \to A_1^*(\lambda^P, E_0)A_2X_f$)

$$\begin{aligned} W_{1,2}(\nu,q^2) &= \hat{W}_{1,2}(q^2)\delta(\nu - E_0),\\ -q^2 &= \frac{w^2}{\gamma^2} + 2\frac{wE_0}{\gamma} + \frac{E_0^2}{\gamma^2} + q_\perp^2,\\ \hat{W}_1 &= 2\pi[|T^e|^2 + |T^m|^2],\\ \hat{W}_2 &= 2\pi\frac{q^4}{(E_0^2 - q^2)^2}\\ &\times\left[2|M^{\mathrm{C}}|^2 - \frac{E_0^2 - q^2}{q^2}(|T^e|^2 + |T^m|^2)\right]. \end{aligned} \tag{6}$$

See notations again in [3].

We neglect the transverse electric T^e and transverse magnetic T^m matrix elements compared to the Coulomb one $M^{\mathrm{C}} \equiv M_\lambda$ for $0^+ \to \lambda^P$ nuclear transitions. Then for the "inelastic" photon process with a nuclear discrete state excitation we get

$$n_1^{(\lambda)}(w) = \frac{4\alpha}{\pi}\int \mathrm{d}^2 q_\perp \frac{q_\perp^2}{(E_0^2 - q^2)^2}|M_\lambda(-q^2)|^2, \tag{7}$$

where $M_\lambda(q)$ is the inelastic nuclear form factor and $-q^2 = q_L^2(w) + q_\perp^2$.

The equivalent photon number (7) can be represented as function of $q_\perp$ for inelastic photon emission:

$$\begin{aligned} \frac{\mathrm{d}n_1^{(\lambda)}}{\mathrm{d}q_\perp^2}(w_1, q_\perp) &= \frac{4\alpha}{\pi}\frac{q_\perp^2}{(E_0^2 - q^2)^2}|M_\lambda(-q^2)|^2 =\\ &= \frac{4\alpha}{\pi}\left|\frac{q_\perp}{(E_0^2 - q^2)}M_\lambda(-q^2)e^{i\varphi_\perp}\right|^2, \end{aligned} \tag{8}$$

where $q_\perp e^{i\varphi_\perp} = \mathbf{q}_\perp$ (see [12]).

Let us do the inverse transformation to the impact parameter b presentation:

$$f(\mathbf{b}) = \frac{1}{2\pi}\int \mathrm{d}^2 q_\perp e^{-i\mathbf{q}_\perp\mathbf{b}} f(\mathbf{q}_\perp). \tag{9}$$

For the function under the module in eq. (8) we get

$$\begin{aligned} f(\mathbf{b}) &= \frac{1}{2\pi}\int \mathrm{d}^2 q_\perp \frac{q_\perp}{(E_0^2 - q^2)} M_\lambda(-q^2)e^{i\varphi_\perp}\cdot e^{-i\mathbf{q}_\perp\mathbf{b}} =\\ &= i\int \mathrm{d}q_\perp \frac{q_\perp^2}{(E_0^2 - q^2)} M_\lambda(-q^2)\cdot J_1(q_\perp b) =\\ &= \frac{i}{b}\int \mathrm{d}u \frac{u^2}{u^2 + (E_0^2 + q_L^2)\, b^2}\\ &\times M_\lambda\left(-\frac{x^2 + u^2}{b^2}\right) J_1(u). \end{aligned} \tag{10}$$

Here $x = q_L b = wb/\gamma_A$ and $u = q_\perp b$.

If we take $M_{\rm el}$ instead of the inelastic M_λ as

$$|M_{\rm el}(-q^2)|^2 = \frac{Z^2}{4\pi} F_{\rm el}^2(-q^2) \qquad (11)$$

and put $E_0 = 0.0$, then we get a well-known formula of the impact parameter-dependent equivalent photon number of the A_2 nucleus (see (4) in [12]):

$$N_2^{(\rm el)}(w,b) = \frac{Z^2\alpha}{\pi^2}\frac{1}{b^2}\cdot \cdot\left|\int {\rm d}u \frac{u^2}{x^2+u^2} J_1(u) F_{\rm el}[-(x^2+u^2)/b^2]\right|^2, \qquad (12)$$

For a point charge, $F_{\rm el}(q) \equiv 1$, we readily obtain

$$N_2^{(\rm el)}(w,b) = \frac{Z^2\alpha}{\pi^2}\frac{1}{b^2}\, x^2\ K_1^2(x), \qquad (13)$$

in agreement with [3] at very large γ_A.

We write the form factors of the elastic and inelastic nuclear process in the same forms:

$$\mathcal{F}_\lambda^2(q) \;=\; \frac{1}{4\pi e^2 Z^2} F_\lambda^2(q)\,, \qquad (14)$$

$$F_0^2(q) \;=\; \left|4\pi\frac{1}{q}\int \sin(qr)\rho_0(r) r {\rm d}r\right|^2_{q\to 0} \to 1\,, \qquad (15)$$

$$F_\lambda^2(q) \;=\; (2\lambda+1)\left|4\pi\int j_\lambda(qr)\rho_\lambda(r,Z) r^2 {\rm d}r\right|^2_{q\to 0} \qquad (16)$$

$$\to \frac{(4\pi)^2 B(E\lambda)}{e^2 Z^2 [(2\lambda+1)!!]^2}\; q^{2\lambda}, \qquad (17)$$

where $\rho_\lambda(r,Z)$ is the nuclear transition density and $B(E_0\lambda)$ is the reduced transition probability .

Then for the matrix elements M_λ we get, in the limit $q \to 0$,

$$|M_{\rm el}(-q^2)|^2 = \left(\frac{Z^2}{4\pi}\right) F_{\rm el}^2(q)\,\Big|_{q\to 0} \to \frac{Z^2}{4\pi}\,, \qquad (18)$$

$$|M_\lambda(-q^2)|^2 = \left(\frac{Z^2}{4\pi}\right) F_\lambda^2(q)|_{q\to 0} \to \left(\frac{Z^2}{4\pi}\right)\frac{(4\pi)^2 B(E_0\lambda)}{e^2 Z^2[(2\lambda+1)!!]^2} q^{2\lambda}. \qquad (19)$$

The equivalent photon number for the inelastic process with A_1 nuclear transition $0 \to \lambda$ will be

$$N_1^{(\lambda)}(w,b) = \frac{Z^2\alpha}{\pi^2}\frac{1}{b^2} \times\left|\int_0^\infty {\rm d}u \frac{u^2}{x_{\rm in}^2+u^2} J_1(u) F_\lambda[-(x_{\rm in}^2+u^2)/b^2]\right|^2, \qquad (20)$$

as the generalization of (12). Here $x_{\rm in}^2 = (E_0^2 + \frac{w^2}{\gamma^2} + 2\frac{wE_0}{\gamma} + \frac{E_0^2}{\gamma^2})\ b^2$.

We take the inelastic form-factor from inelastic electron scattering off nuclei. A good parameterization of the inelastic form-factor is

$$F_\lambda^2(q) = 4\pi\beta_\lambda^2 j_\lambda^2(qR) e^{-q^2 g^2} \qquad (21)$$

in Helm's model [13]. The squared transition radius is equal to $R_\lambda^2 = R^2 + (2\lambda+3)g^2$, where R and g are the model parameters.

According to (19) the reduced transition probability in this case is equal to

$$B(E_0\lambda) = \frac{\beta_\lambda^2}{4\pi} Z^2 e^2 R^{2\lambda}. \qquad (22)$$

So, the formulae for the process (1) are

$${\rm d}\sigma_{A_1A_2\to A_1^*A_2X_f} = \int\frac{{\rm d}w_1}{w_1}\int\frac{{\rm d}w_2}{w_2} n_1^{(\lambda)}(w_1) n_2(w_2)\ \cdot \cdot\,{\rm d}\sigma_{\gamma\gamma\to X_f}(w_1,w_2); \qquad (23)$$

$$n_1^{(\lambda)}(w_1) = \frac{Z^2\alpha}{\pi^2}\int {\rm d}^2 q_\perp \frac{q_\perp^2}{(E_0^2 - q_{\rm in}^2)^2}\ \cdot \cdot\,|F_\lambda(-q_{\rm in}^2)|^2; \qquad (24)$$

$$-q_{\rm in}^2 = \frac{w^2}{\gamma_A^2} + 2\frac{wE_0}{\gamma_A} + \frac{E_0^2}{\gamma_A^2} + q_\perp^2; \qquad (25)$$

$$n_2(w_2) = \frac{Z^2\alpha}{\pi^2}\int {\rm d}^2 q_\perp \frac{q_\perp^2}{q_{\rm el}^4} F_{\rm el}^2(-q_{\rm el}^2); \qquad (26)$$

$$-q_{\rm el}^2 = \left(\frac{w}{\gamma_A}\right)^2 + q_\perp^2. \qquad (27)$$

The value $q_{\rm in}^2$ is close to $q_{\rm el}^2$ at a large γ_A factor at LHC energies.

The effective two-photon luminosity can be expressed as

$$L(\omega_1,\omega_2) = 2\pi\int_{R_1}^\infty b_1{\rm d}b_1\int_{R_2}^\infty b_2{\rm d}b_2\int_0^{2\pi}{\rm d}\phi\ \cdot \cdot\,N_1^{(\lambda)}(\omega_1,b_1) N_2^{(\rm el)}(\omega_2,b_2)\Theta(B^2), \qquad (28)$$

where R_1 and R_2 are the nuclear radii, $\Theta(B^2)$ is the step function and $B^2 = b_1^2 + b_2^2 - 2b_1b_2\cos\phi - (R_1+R_2)^2$ [3]. Then the final cross-section is

$$\sigma_{A_1A_2\to A_1^*A_2X_f} = \int\frac{{\rm d}\omega_1}{\omega_1}\int\frac{{\rm d}\omega_2}{\omega_2} L(\omega_1,\omega_2)\ \sigma_{\gamma\gamma\to X_f}(w_1,w_2)\,. \qquad (29)$$

2 Nuclear levels and form factors

The elastic form factor of a light nucleus is

$$F_{\rm el}(q^2) = \exp\left(-\frac{\langle r^2\rangle}{6}\ q^2\right) \qquad (30)$$

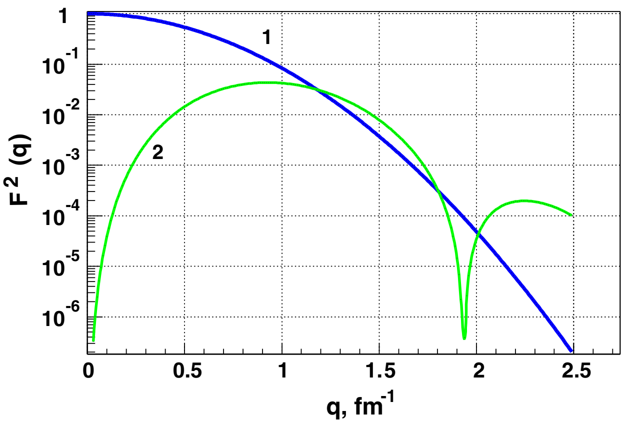

Fig. 2. The elastic form factor (1) of ^{16}O and the inelastic form factor (2) of ^{16}O $(2^+, 6.92$ MeV) from the electron scattering.

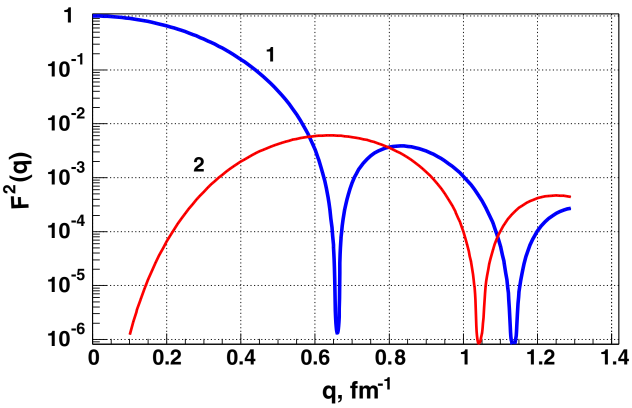

Fig. 3. The elastic form factor (1) of ^{208}Pb and the inelastic form factor (2) of ^{208}Pb $(3^-, 2.615$ MeV).

with $\sqrt{\langle r^2 \rangle} = 2.73$ fm for the nucleus ^{16}O. For a heavy nucleus we take a modified Fermi nuclear density [14]

$$\rho(r) = \rho_0 \left\{ \frac{1}{1+\exp\left(\frac{-r-R}{g}\right)} + \frac{1}{1+\exp\left(\frac{r-R}{g}\right)} - 1 \right\} = \rho_0 \, \frac{\sinh(R/g)}{\cosh(R/g)+\cosh(r/g)}, \qquad (31)$$

$$\rho_0 = \frac{3}{4\pi R^3} \left\{ 1 + \left(\frac{\pi g}{R}\right)^2 \right\}^{-1}, \qquad (32)$$

with the parameters for ^{208}Pb equal to $R = 6.69$ fm and $g = 0.545$ fm. This form of the density is close to the usual Fermi density at $g \ll R$

$$\rho_{\rm F}(r) = \rho_0 \, \frac{1}{1+\exp\left(\frac{r-R}{g}\right)} \qquad (33)$$

and allows us to calculate the elastic form factor analytically:

$$F_{\rm el}(q) = \frac{4\pi^2 R g \rho_0}{q \sinh(\pi g q)} \left\{ \frac{\pi g}{R} \sin(qR) \coth(\pi g q) - \cos(qR) \right\}. \qquad (34)$$

There are a few discrete levels of ^{16}O below the α, p and n thresholds $E_{\rm th}(\alpha) = 7.16$ MeV, $E_{\rm th}(p) = 12.1$ MeV, $E_{\rm th}(n) = 15.7$ MeV [15]. The level 2^+ at $E_0 = 6.92$ MeV is the strongest excited one in the electron scattering.

The parameters from the inelastic electron scattering fit on ^{16}O with excitation of 2^+ level ($E_0 = 6.92$ MeV) are [16]

$$\beta_2 = 0.30, \quad R = 2.98 \text{ fm}, \quad g = 0.93 \text{ fm}.$$

They correspond to

$$B(E_0 2) = (36.1 \pm 3.4) e^2 \text{ fm}^4 . \qquad (35)$$

There are more than 70 discrete levels of ^{208}Pb [17] below the neutron threshold $E_{\rm th}(n) = 7.367$ MeV. About 30% of the levels decay to the first 3^- level of ^{208}Pb at $E_0 = 2.615$ MeV. This level is well studied experimentally [18] and has a large excitation cross-section.

The reduced transition probability from the fit of the inelastic electron scattering on ^{208}Pb with excitation of the 3^- level is [18]

$$B(E_0 3) = (6.12 \; 10^5 \pm \; 2.2\%) e^2 \text{ fm}^6 .$$

We calculate the parameter β_3, using this $B(E_0 3)$, and take R and g from the density of the ^{208}Pb ground state:

$$\beta_3 = 0.113, \quad R = 6.69 \text{ fm}, \quad g = 0.545 \text{ fm}.$$

Note that there are many levels higher than $E_0 = 2.615$ MeV which decay to the first level of ^{208}Pb. This fact increases the event rate of the process (1), but we do not know the excitation cross-section of these levels.

The elastic form factor (30) of ^{16}O and the inelastic form-factor of ^{16}O $(2^+, 6.92$ MeV) (21), corresponding to the electron scattering data, are shown in fig. 2. The same for a nucleus ^{208}Pb and the excited state ^{208}Pb $(3^-, 2.64$ MeV) are shown in fig. 3.

The squared inelastic form factor is less than the elastic form factor by more then two orders at small $q < q_0$ ($q_0 = 0.5$ fm^{-1} for ^{16}O and $q_0 = 0.4$ fm^{-1} for ^{208}Pb). In the region of $q > q_0$ they are comparable. The region of large $q > q_0$ will contribute to the small impact parameter b. We are able to calculate the photon luminosity (28) for all regions of b to get the maximum electromagnetic cross-section of the process we are interested in. Then it should be possible to compare with experimental data in condition of clear selection of such process by the photon signal and the veto neutron or proton signal in the ZDC.

3 Angular and energy distributions of secondary nuclear photons

We suppose that the nucleus $A_1^*(\lambda\mu)$ in process (1) is unpolarized. At this point now we do not know the relative excitation probability of $|\lambda\mu\rangle$ states, where μ is a projection of spin λ. This assumption needs further study in the

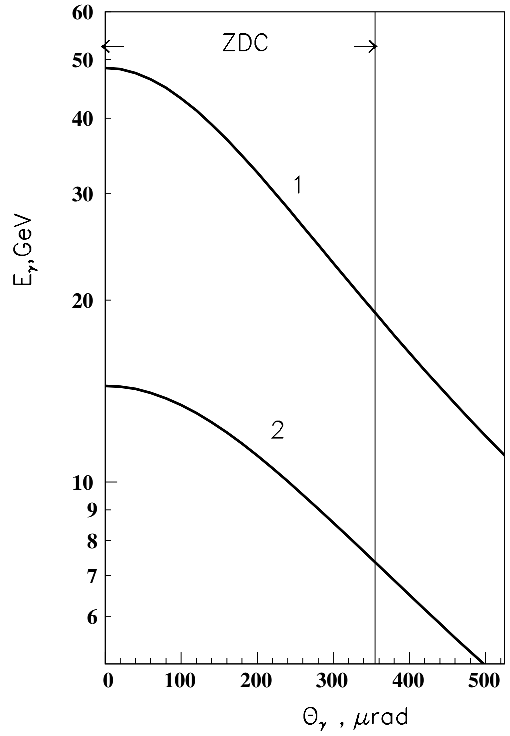

Fig. 4. Nuclear photon energy as function of its polar angle in the laboratory system at LHC energies for two nuclei: ^{16}O $(2^+ \to 0^+, 6.92\ \mathrm{MeV})$ (1) and ^{208}Pb $(3^- \to 0^+, 2.615\ \mathrm{MeV})$ (2). ZDC marks the region of the zero-degree calorimeter in the CMS.

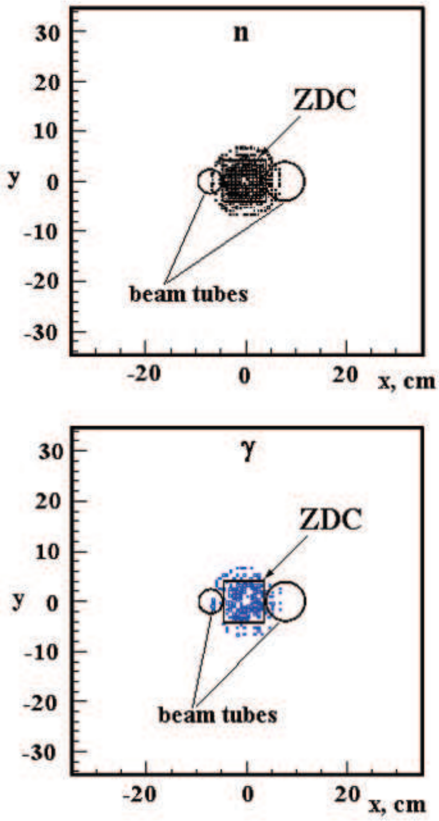

Fig. 5. Transverse ZDC plane. The points are the simulated hits of neutrons (top) and photons (bottom) from ref. [21].

future. So we use a formula (27) in our work [10] for the angular distribution of secondary photons, which is valid for isotropic photon distribution in the rest system of A_1^* according to equal probabilities of excitation.

If we calculate the integral cross-section of reaction (1) using eq. (29), then the angular and energy distribution of photons are equal to [10]

$$\frac{\mathrm{d}\sigma_{A^*}}{\mathrm{d}\theta_\gamma} = \sigma_{A_1A_2\to A_1^*A_2X} \cdot \frac{2\gamma_{A_1^*}^2 \sin\theta_\gamma}{(1+\gamma_{A_1^*}^2 \tan^2\theta_\gamma)^2 \cdot \cos^3\theta_\gamma}, \tag{36}$$

$$\frac{\mathrm{d}\sigma_{A^*}}{\mathrm{d}E_\gamma} = \sigma_{A_1A_2\to A_1^*A_2X} \cdot \frac{\Theta(2\gamma_{A_1^*}E_0 - E_\gamma)}{2\gamma_{A_1^*}E_0}, \tag{37}$$

where $\Theta(x)$ is the step function.

The angular distribution does not depend on the photon energy and the energy distribution is uniform.

The photon energy E_γ and the polar angle θ_γ in the laboratory system are defined as

$$\begin{aligned} E_\gamma &= \gamma_{A_1^*}E_0(1+\cos\theta'_\gamma) \\ &= 2\gamma_{A_1^*}E_0/(1+\gamma_{A_1^*}^2\tan^2\theta_\gamma), \end{aligned} \tag{38}$$

$$\tan\theta_\gamma = \frac{1}{\gamma_{A_1^*}}\ \frac{\sin\theta'_\gamma}{1+\cos\theta'_\gamma}, \tag{39}$$

where θ'_γ and θ_γ are the polar angles of the nuclear photon in the rest nuclear system and in the laboratory system with an axis $\mathbf{z}||\mathbf{p}_{A^*}$. The photon energy E_γ dependence on θ_γ is shown in fig. 4. Thus the energy E_γ will depend on the position of photon hit.

Our calculations with the TPHIC event generator [19] show that a deflection of the direction $\mathbf{p}_{A^*}$ from $\mathbf{p}_{\mathrm{beam}}$ at LHC energies in the reaction (1) is very small at large γ_A, $\langle\Delta\theta\rangle \simeq 0.5\ \mu$rad.

In the experiments CMS and ALICE, which are planned at LHC (CERN), the zero-degree calorimeter [20, 21] was suggested for the registration of nuclear neutrons after ion interaction. We demonstrate a schematic figure of the ZDC CMS at a distance $L = 140$ m in the plane transverse to the beam direction in fig. 5. The CMS group also plans to include the electromagnetic calorimeter in front of the ZDC.

As an example, we show the angular distributions (36) in arbitrary units and the energy dependence (38) on the (x, y) coordinates of the ZDC CMS for the two nuclei ^{16}O and ^{208}Pb in fig. 6. The direction of the nucleus A_1^* coincides here with the beam direction. The point $(x, y) = (0, 0)$ is the center of the ZDC plane.

4 Cross-section of the process with the nuclear γ radiation

We demonstrate our results for the $\eta_c(2.979)$ production. The previous results [3] used old values of the widths and a point nuclear charge. Now we take resonance parameters

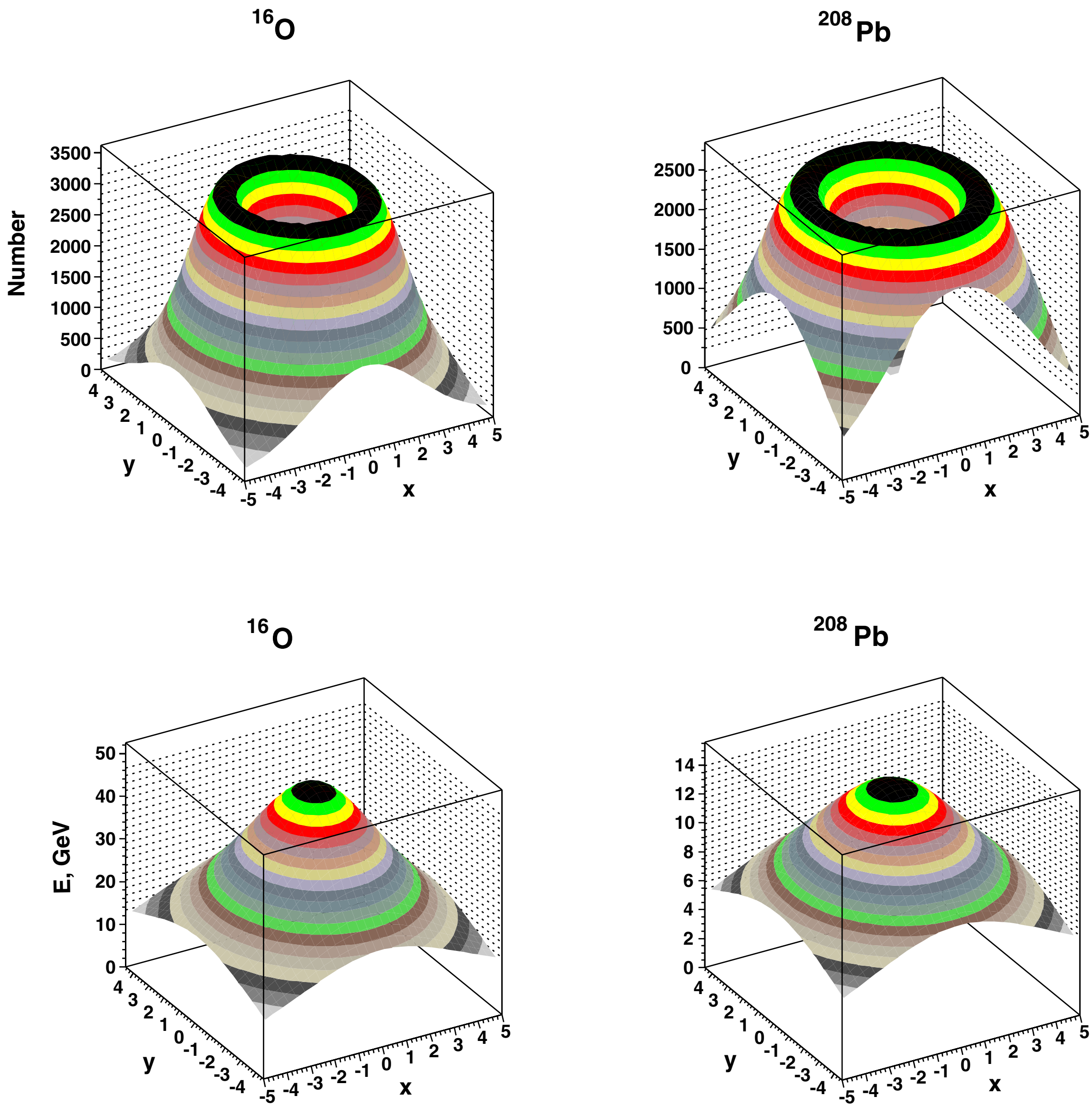

Fig. 6. The photon angular distributions (upper row) and the energy dependence (lower row) for ${}^{16}\mathrm{O}^*(2^+, 6.92\ \mathrm{MeV})$ (left column) and ${}^{208}\mathrm{Pb}^*(3^-, 2.62\ \mathrm{MeV})$ (right column) radiation decay in the laboratory system on the ZDC plane (x, y) at 140 m distance from point interaction. x, (cm) is the horizontal and y, (cm) is the vertical axis. The photon energy interval in the ZDC region is 19–48 GeV for ${}^{16}\mathrm{O}^*(2^+)$ and 7–14 GeV for ${}^{208}\mathrm{Pb}^*(3^-)$.

from the review of particle physics [22], $\Gamma_{\eta_c \to \gamma\gamma} = 4.8$ keV, and a realistic charge distribution. The calculations was made with the help of TPHIC event generator [19].

We use a well-known formula [2] of the narrow resonance cross-section:

$$\sigma_{\gamma\gamma \to X}(w_1, w_2) = 8\pi^2 (2\lambda_X + 1) \Gamma_{X \to \gamma\gamma} \delta(W^2 - M_X^2)/M_X , \tag{40}$$

where $W^2 = 4w_1w_2$, λ_X and M_X is the spin and mass of the resonance. The LHC luminosity and our results according to (29) and (28) are in table 1 for the process (1) with $A_{\mathrm{final}} = A_1$ or A_1^*.

Our results in table 1 show that though the cross-section of the process (1) for the nucleus ^{208}Pb is larger than that for ^{16}O, the event rate is smaller because of the lower LHC luminosity for ^{208}Pb. The cross-section with a nuclear excitation is smaller by three orders of magnitude than that without the excitation, since the intensity of excitation is not large and the inelastic form factor is smaller than the elastic form factor (see figs. 2 and 3). Therefore for the accepted LHC luminosities it is possible to use secondary photons as a signature of clear electromagnetic nuclear processes only for the production X_f with rather large cross-section $\sigma_{\gamma\gamma \to X}$. Light ions are more preferable than heavy ions to detect the nuclear γ radiation.

5 Conclusion

In this work we suggest a new signature of the peripheral ion collisions.

Table 1. Cross-section of $\eta_c(2.979\,\mathrm{GeV})$ production by $\gamma\gamma$ fusion.

A_{final}	L (cm^{-2} s^{-1})	L (pb^{-1})	σ	event/10^6 s
Point charge of the nuclei				
$^{208}Pb_{82}$	$4.2\cdot 10^{26}$	0.00042	356 μb	147000
$^{16}O_8$	$1.4\cdot 10^{31}$	14.0	73 nb	1020000
With form factors of the nucleus and in the region $R < b < \infty$				
$^{208}Pb_{82}$	$4.2\cdot 10^{26}$	0.00042	296 μb	122000
$^{208}Pb^*_{82}$ (3^-)	$4.2\cdot 10^{26}$	0.00042	129 nb	53
$^{16}O_8$	$1.4\cdot 10^{31}$	14.0	66 nb	926000
$^{16}O^*_8$ (2^+)	$1.4\cdot 10^{31}$	14.0	0.201 nb	2810

The formalism of the process (1) is developed in the frame of the equivalent photon approximation. The new point is the introduction of the inelastic nuclear form factor. It allows to consider the excitation of discrete nuclear levels and their following γ radiation decay. It is shown that the energy of this secondary photons are in the GeV region due to a large Lorentz boost at LHC energies. The angular distribution of the photons has a peculiar form as a function of polar angle in the beam direction. The majority of photons fly in the region of angles of a few hundred micro-radians, which are those detactable in the ZDC CMS and ALICE experiments.

Thus the nuclear γ radiation is a good signature of clear peripheral ion collisions at LHC energies when A and Z of the beam ion are conserved. The trigger requirements will include a signal in the central rapidity region of particles from X_f decay, a signal of photons in the electromagnetic detector in front of the zero-degree calorimeter and a veto signal of neutrons in the ZDC. We suggest to use the veto signal of the neutron in order to avoid the processes with nuclear decay into nucleon fragments. The nuclear γ radiation can be used for tagging the events with particle production in the central rapidity region in ultra-peripheral collisions.

Light nuclei are more preferable in comparison with heavy ions, since they have higher beam luminosity at LHC. The cross-sections of the process with the nuclear excitation are three orders of magnitude smaller than the one without excitation. The accepted nuclear luminosities enable us to use this signature for the large cross-section of the X_f system production.

Authors are very grateful to L.I. Sarycheva and S.A. Sadovsky for the useful discussions and K. Hencken and R. Vogt for helpful comments.

References

1. C.A. Bertulani, G. Baur, Phys. Rep. **163**, 299 (1988).
2. G. Baur, K. Hencken, D. Trautmann, J. Phys. G **24**, 1657 (1998).
3. G. Baur *et al.*, Phys. Rep. **364**, 359 (2002).
4. V.P. Goncalves, C.A. Bertulani, Phys. Rev. C **65**, 054905 (2002).
5. M. Greiner, M. Vidovic, G. Soff, Phys. Rev. C **51**, 911 (1995).
6. S.R. Klein, J. Nystrand, R. Vogt, Eur. Phys. J. C **21**, 563 (2001).
7. S.M. Lietti, C.G. Roldao, Phys. Lett. B **540**, 252 (2002).
8. G. Baur *et al.*, CMS Note 1998/009, hep-ph/9904361.
9. V.V. Balashov, V.L. Korotkikh, I.V. Moskalenko, *Proceedings of the 21th ICRC, Adelaide*, Vol. **2** (Univesrity of Adelaide, 1990) p. 416.
10. V.L. Korotkikh, K.A. Chikin, Eur. Phys. J. A **14**, 199 (2002).
11. V.M. Budnev *et al.*, Phys. Rep. **15**, 182 (1975).
12. G. Baur, L.G. Ferreira, Phys. Lett. B **254**, 30 (1991).
13. R. Helm, Phys. Rev. **104**, 1466 (1956).
14. Yu.N. Eldyshev *et al.*, Sov. J. Nucl. Phys. **16**, 282 (1973).
15. P.M. Endt *et al.*, Nucl. Phys. A **633**, 1 (1998).
16. I.S. Gulkarov, Fiz. Elem. Chastits At. Yadra **19**, 345 (1988).
17. M.J. Martin, Nuclear Data Sheets **147**, 203 (1986).
18. D. Goutte *et al.*, Phys. Rev. Lett. **45**, 1618 (1980).
19. K. Hencken *et al.*, *TPHIC, Event generator of two photon interactions in heavy ion collisions*, Protvino, IHEP 96-38, 1996.
20. C. Roland, *Heavy ion physics at the LHC with the compact muon solenoid detector*, nucl-ex/0405015.
21. ALICE Collaboration, *Technical design report of the ZDC*, CERN/LHCC 99-5, 1999.
22. Particle Data Group (K. Hagiwara *et al.*), Phys. Rev. D **66**, 010001 (2002).